ACS APPLIED MATERIALS & INTERFACES

Research Article

www.acsami.org

Anatase TiO_2 Films with Dominant {001} Facets Fabricated by Direct-Current Reactive Magnetron Sputtering at Room Temperature: Oxygen Defects and Enhanced Visible-Light Photocatalytic Behaviors

Jian-Yun Zheng,[†,‡] Shan-Hu Bao,[†] Yu Guo,[†,‡] and Ping Jin*[,†,§]

[†]State Key Laboratory of High Performance Ceramics and Superfine Microstructure, Shanghai Institute of Ceramics, Chinese Academy of Sciences, Shanghai 200050, China

[‡]Graduate School of Chinese Academy of Sciences, Beijing 100049, China

[§]National Institute of Advanced Industrial Science and Technology (AIST), Moriyama, Nagoya 463-8560, Japan

Supporting Information

ABSTRACT: A TiO_2 film with dominant anatase {001} facets is directly prepared by direct-current reactive magnetron sputtering at room temperature without using morphology-controlling agents. The formation mechanism of anatase TiO_2 films with dominant {001} facets is explained by the competition between thermodynamics and ion impinging in the deposition process. The crystalline TiO_2 film shows a superior photocatalytic efficiency for the degradation of Rhodamine B under UV−visible (λ > 250 nm) lights. Furthermore, a comparable photodegradation of Rhodamine B is also found on the TiO_2 film surface by using visible (λ > 420 nm) lights. During film growth, the surface bombarded by high energy of ions yields plenty of oxygen defects, which can enhance the photocatalytic activity of the films irradiated under visible light.

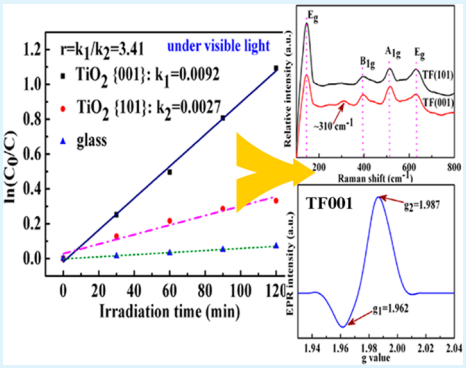

KEYWORDS: *TiO_2 films, oriented anatase {001} facets, room temperature, oxygen defects, enhanced visible-light photocatalytic activity*

1. INTRODUCTION

As a semiconductor photocatalyst, anatase TiO_2 with special orientation has attracted increasing interest in recent years.[1−3] A high percentage of reactive facets in photocatalysts by crystal facet engineering are of the competitive advantages in optimizing photocatalytic reactivity or selectivity.[4−6] Both theoretical and experimental studies show that the {001} facets are much more reactive activities than the {101} facets.[7−10] Unfortunately, anatase TiO_2 crystals are usually dominated by {101} facets, which are thermodynamically stable owing to their lower surface energy (0.44 $J{\cdot}m^{-2}$) than that of {001} facets (0.90 $J{\cdot}m^{-2}$).[11] Since the breakthrough work by Yang et al.,[10] much effort has been dedicated to the fabrication of anatase TiO_2 crystals with a high percentage of exposed {001} facets and to the exploration of these crystals for photocatalytic behavior.[12−16] However, in these cases, the synthesis of anatase TiO_2 with dominant reactive {001} facets involves the use of morphology-controlling agents (MCAs; e.g., fluorine species and diethylenetriamine), which must be eventually removed in order to obtain clean facets. The need for a MCA-free synthesis route stimulates the ongoing research in this field. Currently, significant progress has been made in this field by Amano and co-workers,[17] who reported the fabrication of anatase TiO_2 crystals with dominant {001} facets at a temperature of 1300 °C without using MCAs. However, such a high temperature can give rise to more requirements on equipment and more energy consumption. Apparently, it is highly desirable to develop the preparation of anatase TiO_2 crystals with dominant {001} facets at room temperature in a MCA-free synthesis route. Moreover, most of the photocatalysts are usually in the powdered form, which has to be separated from the water in a slurry system after photocatalytic reaction and is inconvenient for many practical applications. This trouble can be overcome by immobilizing anatase TiO_2 crystals as the film on a substrate.[18]

As mentioned above, the anatase TiO_2 (001) surface is strongly suggested to be more catalytically active than other crystalline phases and facets by several theoretical calculations and experimental results. However, the validity of the enhanced photocatalytic activity of the anatase (001) surface is still controversial; in fact, it is in contrast to some recent experimental observations.[1,3] It can be pointed out by other researchers[3] that the photocatalytic reactivity can be simultaneously tuned through the synergistic effects of absorbance, redox potential, and mobility of charge carriers. Generally, the crystal facets {001} perform a stronger adsorption capacity and

Received: February 16, 2014
Accepted: April 1, 2014
Published: April 10, 2014

   dx.doi.org/10.1021/am500979j | ACS Appl. Mater. Interfaces 2014, 6, 5940−5946

a lower redox potential than other facets owing to their higher density of surface undercoordinated atoms and smaller band gap.[3] Nevertheless, recently, the presence of Ti^{3+} has been suggested to be important for enhancing the photoactivity of (001)-dominant anatase TiO_2 because of the radical species yielded by Ti^{3+} sites.[19] It is thus essential to fully characterize the Ti^{3+} defects of the anatase TiO_2 (001) surface to explicitly identify their effects on the photocatalytic activity. In addition, TiO_2 films have no visible-light response because of their large energy gap of 3.2 eV. The need for effective utilization of solar energy stimulates the ongoing research in this area toward visible-light-responsive TiO_2 films.[12]

Here we report the TiO_2 film with dominant anatase {001} facets (TF001) prepared by direct-current (dc) reactive magnetron sputtering at room temperature without using MCAs. This TiO_2 film exhibits an excellent ability for photodecomposition of Rhodamine B (RhB) under UV−visible and visible light irradiation to the benchmark TiO_2 film with dominant anatase {101} facets (TF101). This result can be closely related with Ti^{3+} defect sites and dominant {001} facets in TF001.

2. EXPERIMENTAL SECTION

A TiO_2 film with dominant anatase {001} facets was directly deposited on n-type Si(100) wafers and plane glass slides by a dc reactive magnetron sputtering system (Shengyang Tengao Vacuum Technology Co. Ltd., JSS-600) with a titanium target (99.99% purity) at room temperature. In the deposition equipment, the angle between the target and the substrate surface normal was fixed at 37° with a substrate rotation of 15 rpm for the deposition process. Prior to loading into the chamber, silicon substrates were ultrasonically cleaned in acetone, deionized water, and ethanol, respectively. Meanwhile, glass substrates were ultrasonically cleaned in a 1.0 mol·L^{-1} sodium hydroxide solution, deionized water, and ethanol, respectively. Then the silicon and glass substrates were placed together in a carrier plate to obtain the film at identical deposition conditions, as described below. It was necessary to point out that the film deposited on silicon substrates was used to analyze its structure, while the film with glass substrates was employed to evaluate its photocatalytic and optical properties. Using a load-lock system, the base pressure of the deposition chamber was kept at 5.0×10^{-5} Pa, and the process pressure was maintained at 2.0 Pa. The target and substrate distances were set at 15 cm. Thereafter, deposition was conducted at a dc power of 700 W (or power density of 8.9 W·cm^{-2}), a deposition time of 2.5 h, a substrate bias of −80 V, and a fixed hybrid gas composed of 35 sccm argon flow rates and 5 sccm O_2 flow rates. Although there was no intentional substrate heating in this experiment, the substrate temperature increased from around 40 to 90 °C during deposition because of bombardment of the energetic particles on the substrate surface. After deposition, the crystalline TiO_2 film with dominant anatase {001} facets was obtained. In addition, the detailed preparation and characterization of a TiO_2 film with dominant anatase {101} facets are described in the Supporting Information (SI).

The chemical composition and valence-band (VB) spectrum of the film surface were analyzed by X-ray photoelectron spectroscopy (XPS) with monochromated Al Kα radiation at a pass energy of 29.4 eV. All binding energies were referenced to the C 1s peak (285.0 eV) arising from adventitious carbon. X-ray diffraction (XRD) measurement was applied to characterize the crystalline structure of the film on a Rigaku Ultima IV diffractometer with grazing-angle mode. Raman measurement was carried out using a HR800 Raman microscopy instrument with a 532 nm argon-ion laser and a resolution of 1 cm^{-1}. The surface morphology of the film was obtained by atomic force microscopy (AFM; SII Nano Technology Ltd., Nanonavi II) in noncontact mode. The thickness and cross-sectional structure of the film were observed by cross-sectional high-resolution transmission electron microscopy (HRTEM; Tecnai G2 F20 S-Twin) with an acceleration voltage of 200 kV applied. Electron paramagnetic resonance (EPR) spectra were taken on a JES FA-200 (JEOL) continuous-wave EPR spectrometer by applying an X band (9.1 GHz) and a sweeping magnetic field at 120 K.

The optical transmittance characteristics were monitored on a Hitachi U-3010 UV−visible−near-IR spectrophotometer at normal incidence from 250 to 2600 nm. The absorption coefficient α relates to the transmittance T and film thickness d as follows:

$$\alpha = -\frac{\ln(T)}{d} \tag{1}$$

The optical energy band gaps of TiO_2 films have been estimated by using the classical relationship of optical absorption:

$$\alpha h\nu = B(h\nu - E_g)^m \tag{2}$$

where B, E_g, and $h\nu$ denote the band-tailing parameter, optical band gap, and photon energy, respectively. The value of m should be 2, a characteristic value for the indirect allowed transition that dominates over optical absorption.

A total of 1.5 mL of a 0.01 M RhB aqueous solution was diluted by 50 mL of deionized water, and then the dilute solution was stirred under darkness for 2 h to achieve adsorption−desorption equilibrium. Subsequently, the solution was injected into a small-size container with a hollow part of $2.5 \times 2.5 \times 1.0$ cm^3 using a 5 mL injector. The schematic diagram of the degradation experiment was shown in a previous work.[20] It needs to be emphasized that TiO_2 films were irradiated with a xenon lamp (power 300 W) for 2 h to decompose pollutants absorbed on their surface prior to degradation. At given irradiation intervals (30 min), the absorption spectrum of the RhB solution was measured by UV−visible spectroscopy with wavelengths from 650 to 400 nm. The concentration of RhB was determined by monitoring the changes in the absorbance maximum at about 550 nm. According to the Lambert−Beer law, the absorbance is proportional to the concentration of a dilute solution, from which the photodegradation percentage is calculated using the formula

$$\eta = \frac{C_0 - C}{C_0} \times 100\% \tag{3}$$

where η is the degradation rate, C_0 the initial concentration of the RhB solution, and C the concentration at a certain irradiation time. In general, the degradation of RhB can be considered as first-order of the dynamical reaction, as follows:

$$\ln\frac{C_0}{C} = kt \tag{4}$$

where k is the reaction rate and t the reaction time. It should be emphasized that photocatalytic tests were implemented in the stable conditions (e.g., 25 °C and a humidity of 45%).

3. RESULTS AND DISCUSSION

The AFM image (shown in the SI) indicates that the surface of a TiO_2 film with dominant anatase {001} facets was composed of flat sheets with widths of 200−250 nm. The root-mean-square (rms) roughness of the film was around 7.76 nm, making known a relatively smooth surface. The XRD peak position of TF001 in Figure 1a presents a little shift toward low angle compared to the anatase phase (space group $I4_1/amd$ (JCPDS No. 21-1272), as marked by a blue dotted line in Figure 1a), implying significant defect-induced distortion in the film. Further analysis of this pattern indicates that the intensity of the (004) diffraction peak of the film was more intense and sharper than that of other peaks, suggesting a preferential growth along the c axis of the anatase lattice. In the previous investigation on XRD patterns, the anatase TiO_2 films own a sole or dominant (001) plane when a (004) diffraction peak or a distinct (004) preferred orientation is observed.[21−24] On the basis of former researches, TF001 could have a preference for

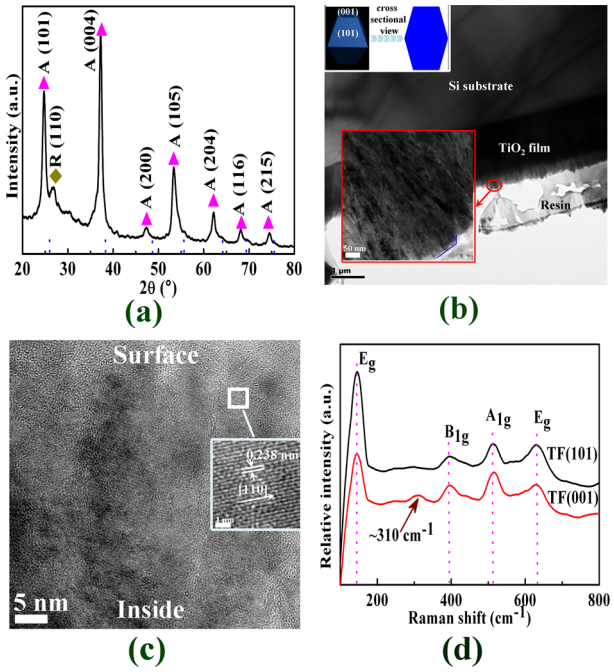

Figure 1. (a) XRD pattern, (b) TEM images (the upper left inset is a schematic of truncated anatase TiO_2, and the bottom left inset corresponds to the red ring with high magnification), and (c) HRTEM images (the inset corresponds to the white box with high magnification) of the TF001. (d) Raman spectra of TF001 and TF101. Therein, A and R denote the anatase and rutile phases in part a, respectively.

the (001) plane. In addition, it should be noted that a slight (110) rutile diffraction peak was also found in the pattern, which could be attributed to the high energy of positive ions, leading to nucleation of the rutile phase.[25] TEM images of TF001 in Figure 1b exhibit that the film had a dense and continuous columnar structure oriented highly perpendicular to the surface of the substrate[26] and the film thickness was 1.85 μm at a deposition time of 2.5 h. Regarding the morphology of {001} facet-dominated anatase TiO_2, a truncated bipyramid has been confirmed,[27] as shown in the upper left of Figure 1b. It can be revealed from the bottom-left inset in Figure 1b that the top of the columnar crystal was planar (marked by blue lines), in line with a cross-sectional view of the truncated bipyramid. To identify the exposed facets of the film on the surface, HRTEM was employed to display a surface atomic structure. The HRTEM image in Figure 1c gives lattice fringes with spacing of 0.238 nm on the film surface, which is assigned to the (004) plane of anatase TiO_2. These results indicate that the top surface of TF001 exists a specified amount of (001) facets. Raman spectra were used to preliminarily survey the exerted influence of the percentage of exposed {001} facets on the geometric structure.[28] As shown in Figure 1d, the intensity of the Raman peaks for TF001 was different from that for TF101, although the peaks of both films appeared at 144 (E_g), 394 (B_{1g}), 514 (A_{1g}), and 636 (E_g) cm^{-1} corresponding to three Raman modes of anatase TiO_2. It has been generally known that the E_g, B_{1g}, and A_{1g} modes are generated by the symmetric stretching vibration of O−Ti−O, symmetric bending vibration of O−Ti−O, and antisymmetric bending vibration of O−Ti−O, respectively. Usually, the surface of the regular TiO_2 with dominant {101} facets consists of saturated 6c-Ti and 3c-O and unsaturated 5c-Ti and 2c-O, while TiO_2 with highly exposed {001} facets only shows the unsaturated 5c-Ti and 2c-O bonding modes on the surface.[10] Therefore, for the surface of a TiO_2 film, the percentage of exposed {001} facets is closely correlated with the number variations of the symmetric stretching vibration and the antisymmetric bending vibration of O−Ti−O; namely, the intensity ratio of the E_g and A_{1g} peaks in the Raman spectra can approximately determine the percentage of exposed {001} facets, as reported by other researchers.[28] Table 1 lists the percentage of exposed {001}

Table 1. Intensity (Area) of the Raman Peaks and Percentage of Exposed {001} Facets

sample	peak area of E_g/144 cm^{-1} (cm^2)	peak area of A_{1g}/514 cm^{-1} (cm^2)	percentage of {001} facets (%)
TF001	27445.8	14893.7	54.3
TF101	59651.5	11821.4	19.8

facets for TF001 (54.3%) and TF101 (19.8%). In addition, according to the XRD data, the percentage of {001} facets for the whole TF001 can be about 50% derived directly from the intensity ratio of the (004) diffraction peak and other diffraction peaks, which nearly keeps in step with the result provided by Raman. Interestingly, besides the above four typical Raman peaks of anatase TiO_2, an unanticipated peak for TF001 appears at 310 cm^{-1} in Figure 1d. In the previous investigation on Raman spectra of TiO_2, it has been pointed out that the oxygen deficiency can result in a new weak mode at wavenumbers higher than 300 cm^{-1}.[29] With respect to the presence of oxygen deficiency, the detailed work will be implemented in the following section.

The key to controlling the anatase TiO_2 crystals with dominant crystallographic facets is to change the relative stability of each facet during deposition, which is intrinsically determined by the competition between thermodynamics and ion impinging. If a film is prepared by a deposition process in the absence of high energy of ion bombardment, the preferred orientation is often determined by the thermodynamic parameter. It is generally known that the crystal plane with lowest surface free energy will be grown preferentially to keep the thermodynamic stability. As a consequence, the TiO_2 films usually exhibit a (101) preferred orientation because of the lowest surface free energy. However, when a high power density or current density (such as 8.9 $W{\cdot}cm^{-2}$ or 22.0 $mA{\cdot}cm^{-2}$) and a considerable substrate bias (such as −80 V) are imposed on the target and substrate (as shown in Figure 2a), respectively, the development of a preferred orientation is also related to the planes with deep ion channeling.[30,31] The density of energy deposition is lower for planes with deep ion channeling than that for other planes. During the deposition process, the radiation damage for these planes is low, and they can serve as seeds for further growth. Like a model proposed by Dobrev,[32] the local high temperature induced by a thermal spike effect causes recrystallization when the high energy of ions bombard the film. The planes with deep channeling directions aligned in the incidence direction of ions can remain the coolest and, accordingly, act as recrystallization centers. Thus, the high deposition energy will change the preferred orientation of the film with deep ion channeling direction along the incidence direction of ions.

In general, the film surface with the highest atomic density exhibits the lowest surface free energy. Figure 2b shows the atomic structures of the (001) and (101) planes in anatase

dx.doi.org/10.1021/am500979j | ACS Appl. Mater. Interfaces 2014, 6, 5940−5946

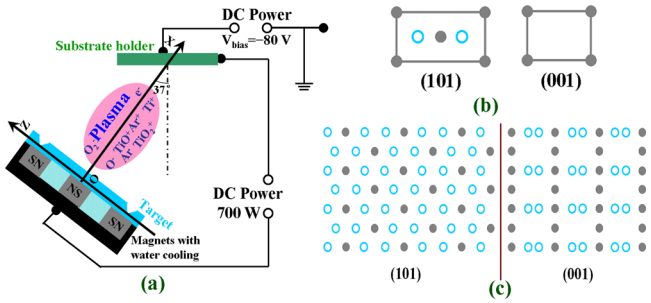

Figure 2. (a) Schematic diagram of a dc reactive magnetron sputtering configuration. (b) Atomic structures of the (001) and (101) planes in anatase TiO_2. (c) Projection of the (001) and (101) planes on the surface normal to the ion incident direction. The gray solid and blue hollow spheres represent titanium and oxygen elements in both parts b and c, respectively.

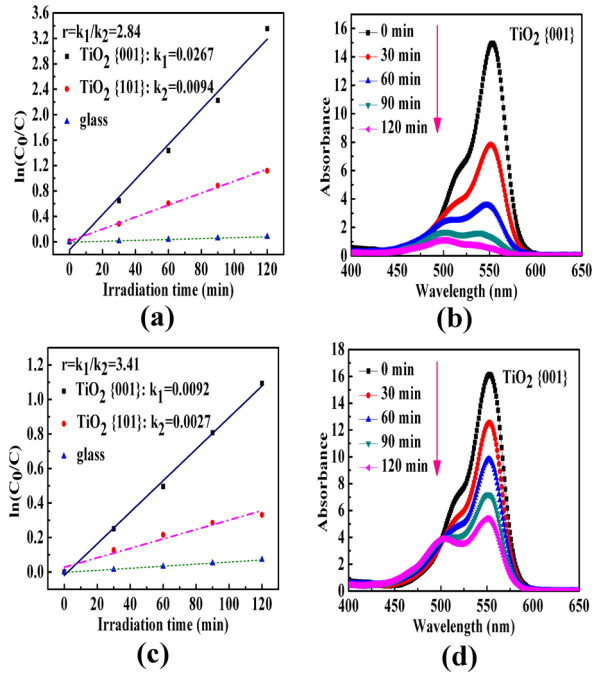

Figure 3. Comparison of the photocatalytic decomposition on TF001 and TF101 under UV−visible (a) and visible (c) light irradiation; variation of the absorption spectra of a RhB aqueous solution degraded by TF001 under UV−visible (b) and visible (d) light irradiation.

TiO_2 related to this work. It is easily observed that the TiO_2 films with (001) orientation have higher surface free energy than those with (101) orientation because of loose atomic arrangement in the (001) plane. In thermodynamics, the (001) orientation of anatase TiO_2 is unstable, leading to it hardly existing in the film surface. However, the bombarding ions can avoid meeting the atoms because of deep ion channeling, which reduces the radiation damage for these crystallites. The crystallites grown on the substrate are projected on the surface normal to the incidence direction of ions (37° to the substrate, as shown in Figure 2a) in order to find wider channels. It can be seen that the (101) plane is densely packed and the (001) plane parallel to the substrate surface offers wider channels for bombarding ions in Figure 2c. When the film is impinged with high energy of ions, the radiation damage for crystallites with {001} planes [e.g., (004)] will be less than for that with {101} planes [e.g., (101)]. Less damage can be produced in crystallites with {001} planes than with {101} planes and other planes. Therefore, the crystallites with {001} facets preferentially grow, replacing the crystallites with {101} facets, as shown in Figure 1.

The UV−visible and visible light photocatalytic activity of a TiO_2 film with dominant anatase {001} facets was evaluated by photodegradation of RhB. As shown in Figure 3a,c, the photodegradation process of RhB was faster on TF001 than on TF101 (its structure is given in the SI) under both UV−visible and visible light irradiation. It was emphatically pointed out that the degradation rate of RhB on TF001 irradiated under visible light was nearly equal to that on TF101 irradiated under UV−visible light. This indicated that the photocatalytic activity of TF001 was considerable under visible light irradiation. However, the degradation rate of RhB was faster under UV−visible light than under visible light, of which the ratio was around 3 for each film. Parts b and d of Figure 3 show the change in absorption spectra recorded for the RhB aqueous solution/TiO_2 film with dominant anatase {001} facets under UV−visible and visible light irradiation as a function of the irradiation time, respectively. After an irradiation time of 120 min, RhB on TF001 was almost completely degraded under UV−visible light irradiation and remained one-third of the concentration under visible light irradiation. In addition, to further measure the photocatalytic activity of both films, the turnover frequency (TOF) and turnover number (TON) were calculated by their definitions. TOF is equal to the number of reactant molecules converted per minute per catalytic site for given reaction conditions, and TON results from multiplication of TOF and the lifetime of the catalyst.[33] The total number of RhB during the testing process is around 1.13×10^{18}, obtained by the concentration of RhB (0.3 mM) and the volume of the reaction container (6.25 mL). The active sites for the thin-film catalyst should be distributed at the top surface of the film with exposure in the solution. In this work, because of the morphology and rms of TF001, we propose roughly that the film surface is made up of a large sum of uniform square pyramids minutely described in the SI. Thus, during the photodegradation process, the number of active sites for TF001 are about 1.35×10^{17} at the reaction interface (area of 6.25 cm^2). After irradiation by UV−visible light for 120 min, the values of TOF and TON are 1.16×10^{-3} s^{-1} and 8.37 for TF001, respectively. These results clearly demonstrate a satisfactory photocatalytic activity of a TiO_2 film with dominant anatase {001} facets under both UV−visible and visible light irradiation. With respect to the reason for the high photocatalytic activity of the film, it will be further discussed in detail below.

With respect to the process of photocatalysis with semiconductor photocatalysts, three mechanistic steps should be involved as follows: excitation, bulk diffusion, and surface transfer of photoexcited charge carriers.[34−36] The photocatalytic reactivity of a TiO_2 film can therefore be simultaneously tuned through the synergistic effects of the absorbance, redox potential, and mobility of charge carriers, which are determined by its electronic band structure and surface atomic structure. Accordingly, the photoactivity of a TiO_2 film with dominant anatase {001} facets must still be related to both its electronic band structure and surface atomic structure. The electronic band structure of TF001 is shown in Figure 4a,b,d. The study of optical absorption gives information about the band structure of compounds.[37,38] Figure 4a demonstrates that the derived band gap from plots of the

dx.doi.org/10.1021/am500979j | ACS Appl. Mater. Interfaces 2014, 6, 5940−5946

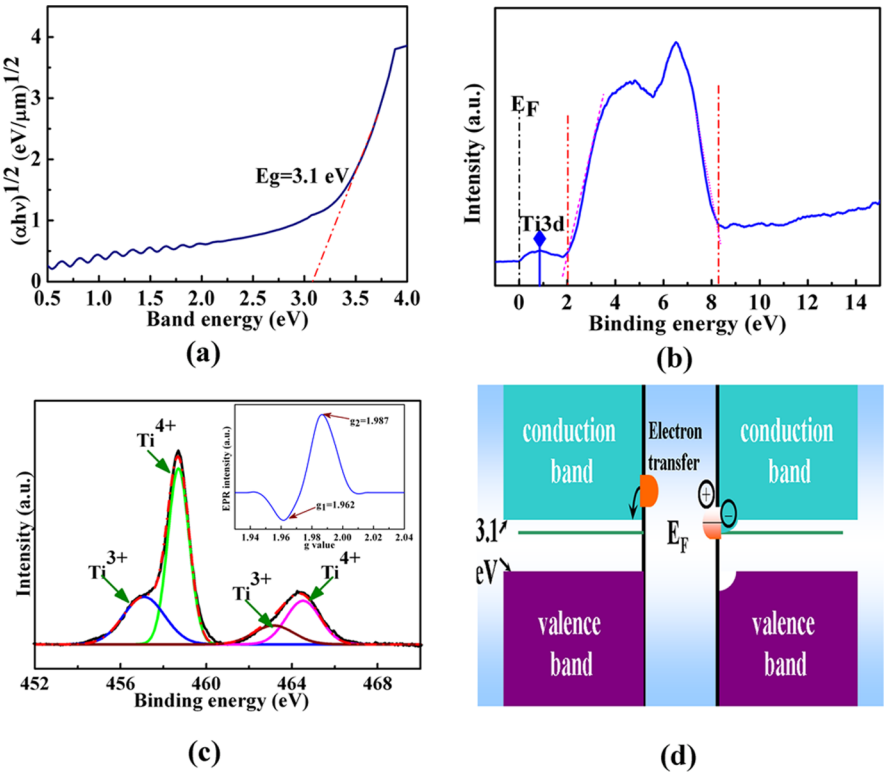

Figure 4. (a) Optical absorption coefficients α as a function of the incident photon energy E for indirect allowed transition for TF001. (b) XPS VB spectrum of TF001. (c) XPS spectrum of Ti 2p of the surface of TF001 (the inset is the EPR spectrum of TF001). (d) Schematic diagram of the band-bending effect due to donor-like surface defect states.

optical absorption coefficients α versus incident photon energy E is 3.1 eV, which is smaller than that of the previous work (3.2 eV).[1,3] This indicates that the intrinsic absorption edge of the TiO_2 film in this work has a definite red shift, leading to an enhanced visible-light photocatalytic activity. The narrow band gap could be ascribed to the presence of the defects (e.g., Ti^{3+} ions or oxygen vacancies).[39] The XPS VB spectrum (Figure 4b) reveals that the VB maximum of the film is at 0.95 eV, which exemplifies the Ti 3d defect states on the surface or subsurface of the film.[40] To further confirm the presence of Ti^{3+}, a typical XPS spectrum of Ti 2p of the film surface is shown in Figure 4c. After deconvolution with a Lorentzian−Gaussian distribution function is performed, the Ti $2p_{3/2}$ spectrum of the film displays two peaks at 458.7 and 457.1 eV, which are assigned to Ti^{4+} and Ti^{3+}, respectively.[19] However, a limited Ti^{3+} doping concentration on the surface only creates localized oxygen vacancy states that deteriorate the electron mobility and exhibit a negligible visible photoactivity.[41] In the theoretical and experimental work reported by other researchers, it is suggested that, with the aim to achieve an efficient activity in the visible spectrum, the concentration of Ti^{3+} must be sufficiently high to induce a continuous vacancy band of electronic states just below the conduction band edge of TiO_2.[41,42] As a result, low-temperature EPR was conducted to identify a certain amount of Ti^{3+} existing in the inner film of TF001. The inset in Figure 4c shows the EPR spectrum of TF001 obtained after exposure to air in the dark for 1 week. Two major features in this spectrum (g_1 = 1.962 and g_2 = 1.987) both belong to the paramagnetic Ti^{3+} centers.[27,43] Because of the instability of Ti^{3+} at the surface of anatase, the EPR result implies that the bulk of Ti^{3+} centers are located in the inner film. From another point of view, the Ti^{3+} defects in the inner film, even in the subsurface, are stable when the film has long-term exposure to air without external stimulation (e.g., bias voltage, illumination).[44] It is reported that the subsurface Ti^{3+} defects in TiO_2 anatase could also contribute to the higher photocatalytic activity because of merging with adsorbed O_2 to form the bridging O_2 dimer.[45] In addition, during the photodegradation process, the subsurface oxygen vacancies (V_O's) caused by Ti^{3+} centers could diffuse to the film surface, leading to the presence of surface V_O's.[44] On the basis of these results, the presence of Ti^{3+} is unambiguously verified in the surface and bulk of TF001. The existence of defect states can substantially cause the band blending effect, as shown in Figure 4d. When defect states are present, the extra electrons in the defects act as donor-like states that create an accumulation layer in the near-surface region. Thus, a downward band bending is formed as a result of an upward shift of the Ti 4d peaks in the VB spectrum.[46] It is necessarily pointed out that the presence of Ti^{3+} has been suggested to be important for the photoactivity of {001}-dominant anatase TiO_2 by previous researchers.[19,47] The reduced titanium-rich defects can be the most active sites for H_2O and O_2 to produce the radical species, which attack the organic molecules (such as RhB) to decompose into the end products. Therefore, the proposed cooperative mechanism of the surface and electronic structures works well for a TiO_2 film with dominant anatase {001} facets. In addition, on the basis of the surface roughness of the film (in Figure 1a) and TF101 (shown in the SI), the order of the photocatalytic activity above is not very consistent with the order of the surface roughness or surface area. Herein, it is believed that the surface area is not the decisive factor influencing the activity of the TiO_2 film in this work.

dx.doi.org/10.1021/am500979j | ACS Appl. Mater. Interfaces 2014, 6, 5940−5946

4. CONCLUSIONS

In summary, a MCA-free and low-temperature synthesis route for the preparation of TiO_2 films with dominant anatase {001} facets is proposed by dc reactive magnetron sputtering. The proposed route is simple and reproducible. The formation of anatase TiO_2 films with dominant {001} facets is explained by the competition between thermodynamics and ion impinging in the deposition process. In addition, because of the presence of Ti^{3+}, TiO_2 films with dominant {001} facets show excellent photocatalytic activity under both UV−visible and visible light irradiation.

■ ASSOCIATED CONTENT

Supporting Information

Detailed sample preparation and structure of TF101 and the morphology and optical properties of TF001. This material is available free of charge via the Internet at http://pubs.acs.org.

■ AUTHOR INFORMATION

Corresponding Author

*E-mail: p-jin@mail.sic.ac.cn.

Notes

The authors declare no competing financial interest.

■ ACKNOWLEDGMENTS

The authors are grateful to the high-tech project of MOST (Grants 2012AA030305, 2012BAA10B03, and 2014AA032802), the national sci-tech support plan, the National Natural Science Foundation of China (Grants 51032008, 51272273, 51102270, 51272271, 51172265, and 51372264), and the Science and Technology Commission of Shanghai Municipality (Grants 13PJ1409000 and 13NM1402200).

■ REFERENCES

(1) Pan, J.; Wu, X.; Wang, L. Z.; Liu, G.; Lub, G. Q.; Cheng, H. M. Synthesis of Anatase TiO_2 Rods with Dominant Reactive {010} Facets for the Photoreduction of CO_2 to CH_4 and Use in Dye-Sensitized Solar Cells. *Chem. Commun.* **2011**, *47*, 8361−8363.

(2) Radović, M.; Salluzzo, M.; Ristić, Z.; Di Capua, R.; Lampis, N.; Vaglio, R.; Granozio, F. M. In Situ Investigation of the Early Stage of TiO_2 Epitaxy on (001) $SrTiO_3$. *J. Chem. Phys.* **2011**, *135*, 034705.

(3) Pan, J.; Liu, G.; Lu, G. M.; Cheng, H. M. On the True Photoreactivity Order of {001}, {010}, and {101} Facets of Anatase TiO_2 Crystals. *Angew. Chem., Int. Ed.* **2011**, *50*, 2133−2137.

(4) Xiang, Q.; Yu, J.; Jaroniec, M. Tunable Photocatalytic Selectivity of TiO_2 Films Consisted of Flower-like Microspheres with Exposed {001} Facets. *Chem. Commun.* **2011**, *47*, 4532.

(5) Fang, W. Q.; Gong, X. Q.; Yang, H. G. On the Unusual Properties of Anatase TiO_2 Exposed by Highly Reactive Facets. *J. Phys. Chem. Lett.* **2011**, *2*, 725−734.

(6) Yang, X. H.; Li, Z.; Liu, G.; Xing, J.; Sun, C. H.; Yang, H. G.; Li, C. Z. Ultra-Thin Anatase TiO_2 Nanosheets Dominated with {001} Facets: Thickness-Controlled Synthesis, Growth Mechanism and Water-Splitting Properties. *CrystEngComm* **2011**, *13* (5), 1378−1383.

(7) Han, X. G.; Kuang, Q.; Jin, M. S.; Xie, Z. X.; Zheng, L. S. Synthesis of Titania Nanosheets with a High Percentage of Exposed (001) Facets and Related Photocatalytic Properties. *J. Am. Chem. Soc.* **2009**, *131*, 3152.

(8) Xiang, Q. J.; Lv, K. L.; Yu, J. G. Pivotal Role of Fluorine in Enhanced Photocatalytic Activity of Anatase TiO_2 Nanosheets with Dominant (001) Facets for the Photocatalytic Degradation of Acetone in Air. *Appl. Catal., B* **2010**, *96*, 557−564.

(9) Yu, J. G.; Qi, L. F.; Jaroniec, M. Hydrogen Production by Photocatalytic Water Splitting over Pt/TiO_2 Nanosheets with Exposed (001) Facets. *J. Phys. Chem. C* **2010**, *114*, 13118−13125.

(10) Yang, H. G.; Sun, C. H.; Qiao, S. Z.; Zou, J.; Liu, G.; Smith, S. C.; Cheng, H. M.; Lu, G. Q. Anatase TiO_2 Single Crystals with a Large Percentage of Reactive Facets. *Nature* **2008**, *453*, 638−641.

(11) Lazzeri, M.; Vittadini, A.; Selloni, A. Structure and Energetics of Stoichiometric TiO_2 Anatase Surfaces (vol 63, art no 155409, 2001). *Phys. Rev. B* **2002**, *65* (11).

(12) Xiang, Q. J.; Yu, J. G.; Wang, W. G.; Jaroniec, M. Nitrogen Self-Doped Nanosized TiO_2 Sheets with Exposed {001} Facets for Enhanced Visible-light Photocatalytic Activity. *Chem. Commun.* **2011**, *47* (24), 6906−6908.

(13) Wang, X. W.; Liu, G.; Wang, L. Z.; Pan, J. A.; Lu, G. Q.; Cheng, H. M. TiO_2 Films with Oriented Anatase {001} Facets and Their Photoelectrochemical Behavior as CdS Nanoparticle Sensitized Photoanodes. *J. Mater. Chem.* **2011**, *21* (3), 869−873.

(14) Yu, J. G.; Dai, G. P.; Xiang, Q. J.; Jaroniec, M. Fabrication and Enhanced Visible-Light Photocatalytic Activity of Carbon Self-Doped TiO_2 Sheets with Exposed {001} Facets. *J. Mater. Chem.* **2011**, *21* (4), 1049−1057.

(15) Jiang, Z. Y.; Kuang, Q.; Xie, Z. X.; Zheng, L. S. Syntheses and Properties of Micro/Nanostructured Crystallites with High-Energy Surfaces. *Adv. Funct. Mater.* **2010**, *20* (21), 3634−3645.

(16) Liao, Y.; Zhang, H.; Que, W.; Zhong, P.; Bai, F.; Zhong, Z.; Wen, Q.; Chen, W. Activating the Single-Crystal TiO_2 Nanoparticle Film with Exposed {001} Facets. *ACS Appl. Mater. Interfaces* **2013**, *5* (14), 6463−6466.

(17) Amano, F.; Prieto-Mahaney, O. O.; Terada, Y.; Yasumoto, T.; Shibayama, T.; Ohtani, B. Decahedral Single-Crystalline Particles of Anatase Titanium(IV) Oxide with High Photocatalytic Activity. *Chem. Mater.* **2009**, *21* (13), 2601−2603.

(18) Pan, F.; Zhang, J. Y.; Zhang, W. W.; Wang, T. M.; Cai, C. Enhanced Photocatalytic Activity of Ag Microgrid Connected TiO_2 Nanocrystalline Films. *Appl. Phys. Lett.* **2007**, *90* (12), 122114.

(19) Wang, Y.; Sun, H. J.; Tan, S. J.; Feng, H.; Cheng, Z. W.; Zhao, J.; Zhao, A. D.; Wang, B.; Luo, Y.; Yang, J. L.; Hou, J. G. Role of Point Defects on the Reactivity of Reconstructed Anatase Titanium Dioxide (001) Surface. *Nat. Commun.* **2013**, *4*.

(20) Zheng, J. Y.; Bao, S. H.; Guo, Y.; Jin, P. TiO_2 Films Prepared by DC Reactive Magnetron Sputtering at Room Temperature: Phase Control and Photocatalytic Properties. *Surf. Coat. Technol.* **2014**, *240*, 293−300.

(21) Wen, C. Z.; Jiang, H. B.; Qiao, S. Z.; Yang, H. G.; Lu, G. Q. Synthesis of High-reactive Facets Dominated Anatase TiO_2. *J. Mater. Chem.* **2011**, *21* (20), 7052−7061.

(22) Chen, S. Ultrahigh Vacuum Metalorganic Chemical Vapor Deposition Growth and In Situ Characterization of Epitaxial TiO_2 Films. *J. Vac. Sci. Technol., A* **1993**, *11* (5), 2419.

(23) Jeong, B. S.; Norton, D. P.; Budai, J. D.; Jellison, G. E. Epitaxial Growth of Anatase by Reactive Sputter Deposition Using Water Vapor as the Oxidant. *Thin Solid Films* **2004**, *446* (1), 18−22.

(24) Marshall, M.; Castell, M. Shape Transitions of Epitaxial Islands during Strained Layer Growth: Anatase $TiO_2(001)$ on $SrTiO_3(001)$. *Phys. Rev. Lett.* **2009**, *102* (14), 146102.

(25) Lobl, P.; Huppertz, M.; Mergel, D. Nucleation and Growth in TiO_2 Films Prepared by Sputtering and Evaporation. *Thin Solid Films* **1994**, *251*, 72−79.

(26) Cheung, S. H.; Nachimuthu, P.; Engelhard, M. H.; Wang, C. M.; Chambers, S. A. N Incorporation, Composition and Electronic Structure in N-Doped $TiO_2(001)$ Anatase Epitaxial Films Grown on $LaAlO_3(001)$. *Surf. Sci.* **2008**, *602* (1), 133−141.

(27) Yu, X.; Kim, B.; Kim, Y. K. Highly Enhanced Photoactivity of Anatase TiO_2 Nanocrystals by Controlled Hydrogenation-Induced Surface Defects. *ACS Catal.* **2013**, *3* (11), 2479−2486.

(28) Tian, F.; Zhang, Y.; Zhang, J.; Pan, C. Raman Spectroscopy: A New Approach to Measure the Percentage of Anatase TiO_2 Exposed (001) Facets. *J. Phys. Chem. C* **2012**, *116* (13), 7515−7519.

(29) Liu, G.; Li, F.; Wang, D. W.; Tang, D. M.; Liu, C.; Ma, X. L.; Lu, G. Q.; Cheng, H. M. Electron Field Emission of A Nitrogen-Doped TiO_2 Nanotube Array. *Nanotechnology* **2008**, *19* (2), 025606.
(30) Smidt, F. A. Use of Ion-Beam Assisted Deposition to Modify the Microstructure and Properties of Thin-Films. *Int. Mater. Rev.* **1990**, *35* (2), 61−128.
(31) Ensinger, W. Growth of Thin-Films with Preferential Crystallographic Orientation by Ion-Bombardment during Deposition. *Surf. Coat. Technol.* **1994**, *65* (1−3), 90−105.
(32) Dobrev, D. Ion-Beam-Induced Texture Formation in Vacuum-Condensed Thin Metal-Films. *Thin Solid Films* **1982**, *92* (1−2), 41−53.
(33) Kozuch, S.; Martin, J. M. L. "Turning Over" Definitions in Catalytic Cycles. *ACS Catal.* **2012**, *2* (12), 2787−2794.
(34) Linsebigler, A. L.; Lu, G. Q.; Yates, J. T. Photocatalysis on TiO_2 Surfaces—Principles, Mechanisms, and Selected Results. *Chem. Rev.* **1995**, *95* (3), 735−758.
(35) Hoffmann, M. R.; Martin, S. T.; Choi, W. Y.; Bahnemann, D. W. Environmental Applications of Semiconductor Photocatalysis. *Chem. Rev.* **1995**, *95* (1), 69−96.
(36) Wu, L.; Jiang, H. B.; Tian, F.; Chen, Z.; Sun, C.; Yang, H. G. $Ti_{0.89}Si_{0.11}O_2$ Single Crystals Bound by High-Index {201} Facets Showing Enhanced Visible-Light Photocatalytic Hydrogen Evolution. *Chem. Commun.* **2013**, *49* (20), 2016−2018.
(37) Al-Ahmad, A. Y. Preparation and Study of Microstructures, Optical Properties and Oscillator Parameters of Titanium(IV) Oxide (TiO_2) Film. *Opt. Spectrosc.* **2012**, *113* (2), 197−203.
(38) Tang, H.; Prasad, K.; Sanjines, R.; Schmid, P. E.; Levy, F. Electrical and Optical-Properties of TiO_2 Anatase Thin-Films. *J. Appl. Phys.* **1994**, *75* (4), 2042−2047.
(39) Carp, O.; Huisman, C. L.; Reller, A. Photoinduced Reactivity of Titanium Dioxide. *Prog. Solid State Chem.* **2004**, *32* (1−2), 33−177.
(40) Wendt, S.; Sprunger, P. T.; Lira, E.; Madsen, G. K. H.; Li, Z. S.; Hansen, J. O.; Matthiesen, J.; Blekinge-Rasmussen, A.; Laegsgaard, E.; Hammer, B.; Besenbacher, F. The Role of Interstitial Sites in the Ti 3d Defect State in the Band Gap of Titania. *Science* **2008**, *320* (5884), 1755−1759.
(41) Grabstanowicz, L. R.; Gao, S.; Li, T.; Rickard, R. M.; Rajh, T.; Liu, D.-J.; Xu, T. Facile Oxidative Conversion of TiH_2 to High-Concentration Ti^{3+}-Self-Doped Rutile TiO_2 with Visible-Light Photoactivity. *Inorg. Chem.* **2013**, *52* (7), 3884−3890.
(42) Justicia, I.; Ordejon, P.; Canto, G.; Mozos, J. L.; Fraxedas, J.; Battiston, G. A.; Gerbasi, R.; Figueras, A. Designed Self-Doped Titanium Oxide Thin Films for Efficient Visible-Light Photocatalysis. *Adv. Mater.* **2002**, *14* (19), 1399−1402.
(43) Zuo, F.; Wang, L.; Wu, T.; Zhang, Z. Y.; Borchardt, D.; Feng, P. Y. Self-Doped Ti^{3+} Enhanced Photocatalyst for Hydrogen Production under Visible Light. *J. Am. Chem. Soc.* **2010**, *132* (34), 11856−11857.
(44) Setvin, M.; Aschauer, U.; Scheiber, P.; Li, Y. F.; Hou, W.; Schmid, M.; Selloni, A.; Diebold, U. Reaction of O_2 with Subsurface Oxygen Vacancies on TiO_2 Anatase (101). *Science* **2013**, *341* (6149), 988−991.
(45) Li, Y. F.; Liu, Z. P.; Liu, L. L.; Gao, W. G. Mechanism and Activity of Photocatalytic Oxygen Evolution on Titania Anatase in Aqueous Surroundings. *J. Am. Chem. Soc.* **2010**, *132* (37), 13008−13015.
(46) Diebold, U. The Surface Science of Titanium Dioxide. *Surf. Sci. Rep.* **2003**, *48* (5−8), 53−229.
(47) Liu, G.; Pan, J.; Yin, L. C.; Irvine, J. T. S.; Li, F.; Tan, J.; Wormald, P.; Cheng, H. M. Heteroatom-Modulated Switching of Photocatalytic Hydrogen and Oxygen Evolution Preferences of Anatase TiO_2 Microspheres. *Adv. Funct. Mater.* **2012**, *22* (15), 3233−3238.